Journal Name

RSCPublishing

ARTICLE

Effect of Fe/Fe_2O_3 loading on catalytic activity of sulfonated single-walled carbon nanohorn for esterification of palmitic acid

Cite this: DOI: 10.1039/x0xx00000x

Received 00th January 2012,
Accepted 00th January 2012

DOI: 10.1039/x0xx00000x

www.rsc.org/

Chantamanee Poonjarernsilp,[*a,b] Noriaki Sano,[a] Nut Sawangpanich,[c] Tawatchai Charinpanitkul[c] and Hajime Tamon[a]

The effect of dispersion of Fe/Fe_2O_3 nanoparticles in sulfonated single-walled carbon nanohorns (SO_3H/SWCNHs) on their catalytic activity for esterification of palmitic acid was investigated. A gas-injected arc-in-water (GI-AIW) method was employed to synthesize SWCNHs dispersed with iron nanoparticles (Fe-SWCNHs) initially. The Fe-loading amount in Fe-SWCNHs was varied by changing the number of Fe wires inserted in an anode. The results showed that Fe-loading amount was proportionally increased from 6 to 13 wt% with increasing the number of the Fe wires. The surface of Fe-SWCNH was functionalized with acid functional group by sequential two steps: an impregnation of sulphuric acid and a calcination in air. From the characterization results, their acid site concentration was estimated to be 5.6-8.5 mmol g^{-1}, suggesting that the catalyst was a super acid solid catalyst. XRD analyses detected that most of Fe was transformed to α-Fe_2O_3. The catalytic activity of SO_3H/Fe-SWCNHs for esterification of palmitic acid was evaluated to investigate the influence of the Fe-loading on their catalytic activity. The results showed that the yield of methyl palmitate was significantly enhanced by increase of Fe-loading amount. It was discovered that the catalytic activity and the magnetic susceptibility of SO_3H/Fe-SWCNHs can be preserved during the repeated use when the amount of Fe-loading amount is large enough.

Introduction

The increasing demand for fossil fuels gives rise to environmental concerns such as emission of large amount of CO_2, causing the global warming. Against this issue, several alternatives have been proposed, such as solar energy, biomass, and biodiesel.[1-3] Biodiesel is a renewable and environmental friendly alternative to petroleum-based diesel.[4] Biodiesel is a mono alkyl ester of fatty acid produced from vegetable oil or animal fat[5] that contains saturated hydrocarbons (triglycerides) and free fatty acid (FFA).[6]

Transesterification [7, 8] of triglycerides and esterification of FFA are the best schemes for producing high quality biodiesel. All fatty acid sources such as animal fats or plant lipids can be used in biodiesel production. However, the production of biodiesel from human nutrition source can cause a food crisis. Therefore, the majority of researchers have been focusing on non-edible oil or waste cooking oil as a low cost feedstock for biodiesel production.[9-11]

In order to use non-edible oil for biodiesel production, the amount of FFA in oil should be concerned because such kind of oil has high concentration of FFA, for example Jatropha seed oil consists of 48% of oleic acid and 34% of linoleic acid.[12] Such high amount of FFA can cause side reaction with alkaline catalysts, so called saponification. Conversely, the acid catalysts possess advantage in insensitivity to FFA for saponification.[13, 14] It can be used with low cost oil containing high FFA. However, the conventionally-used liquid acid catalyst such as sulphuric acid is corrosive so that special care is necessary to preserve the reaction systems. In addition, such liquid catalyst has drawback to its recovery.

The solid acid catalysts, including sulfonated carbon-based materials,[14-16] are considered as the candidates of potential substitution for liquid acid catalysts due to their characteristics, such as high corrosion resistance and ability to recover and reuse.[17] Ideally, the solid acid catalyst should have the characteristics of interconnected pores with large surface area,[18] a high concentration of strong acid sites and hydrophobic surface to prevent the deactivation by water.[19]

Various types of solid acid catalysts such as ion exchange resins,[20] sulphate oxide,[21] mixed oxides and derivatives[22] and

[a] Department of chemical engineering, Graduate school of engineering, Kyoto University, Nishikyo-ku, Kyoto, 615-8510, Japan.
[b] Department of chemical engineering, Faculty of Engineering, Rajamangala University of Technology Krungthep, Sathorn, Bangkok, 10120, Thailand.
[*] Corresponding author: Fax: 66 2287 9734; Tel: 66 2287 9734;
E-mail address: chantamanee.w@rmutk.ac.th
[c] Faculty of engineering, Chulalongkorn University, Bangkok, 10330, Thailand.

carbon-based acid solid catalysts[15, 16, 23] have been studied. Recently, a novel sulfamic-acid-functionalized iron (iron/iron-oxide core shell) nanoparticles has been reported[23]. The presence of iron/iron-oxide core shell nanoparticles enhanced the catalytic activity on ring opening of expoxidized soybean oils and the recovery of catalysts by magnetic force[17, 24, 25]. It was also reported that iron-oxide nanoparticels can adsorb FFA from vegetable oil, which can promote the adsorption of FFA on catalyst surface[24]. Thus, solid acid catalyst hybridized with iron oxide nanoparticles should achieve high performance of ideal solid catalyst for esterification of FFA. However, the work on the effect of iron oxide on catalytic activity of solid acid catalysts has not yet been studied so far.[23, 24, 26]

In this work, we propose to use single-walled carbon nanohorns (SWCNHs). SWCNHs are kinds of the carbon nanomaterials, and have the suitable properties to meet the requirements of ideal solid acid catalyst. SWCNHs have high resistance against chemicals, suitable pore sizes, thermal stability and hydrophobic surface in nature.[27] Moreover, it is possible to synthesize SWCNHs hybridized with metal nanoparticles by a one-step arc discharge technique.[28, 29] Here, the synthesis condition of SWCNHs dispersed with Fe nanoparticles (Fe-SWCNHs) was first investigated focusing the amount of Fe-loading on the products to provide a suitable structure. Next, the catalysts were prepared using the Fe-SWCNHs by an impregnation method with a subsequent calcination step, and their catalytic activity was evaluated by testing an esterification of palmitic acid. Furthermore, the effect of Fe-loading in catalyst preparation on the catalytic activity was studied.

Results and discussion

Effect of Fe-wire number in synthesis process on morphologies of Fe-SWCNHs: Dispersion of Fe nanopartiles and Fe-loading weight

As explained in the experimental section, the Fe-loading amount in Fe-SWCNHs can be varied by changing the number of Fe wire inserted in a hollow graphite anode in the gas-injected arc-in-water (GI-AIW) [30] method. The transmission electron microscope (TEM) images of Fe-SWCNHs synthesized with varied wire number are shown in Fig. 1(a-d). These figures suggest that the Fe nanoparticles indicated by the dark spots can be formed simultaneously with SWCNHs by this method, and they are highly dispersed in SWCNHs. The analysis by X-ray diffraction (XRD) confirmed that they were non-oxidized Fe as explained later.

The arc plasma at the anode tip can increase the plasma temperature to approximately 5000 K,[31] and the vapors of carbon and Fe emitted from the anode can be quenched during their transfer to cold water. SWCNHs and Fe nanoparticles are then simultaneously formed from these vapors by self-assemble mechanism. A previous article reported that the most of the metallic nanoparticles dispersing in SWCNHs synthesized by this method should be migrated in SWCNHs.[29] Such structure may contribute to avoid merging of metallic nanoparticles when they are calcined.

Though the particle sizes tend to be larger with the increase of Fe-wire number in GI-AIW method, it can be regarded that this change is not significant so that the high dispersion of the Fe nanoparticles whose diameter range in 1-11 nm can be preserved in the present conditions (Fig. 1(f)). It should be noted that the number density of the Fe nanoparticles in Fe-SWCNHs seemed to be higher when the Fe-wire number was increased. This tendency is reasonable because the increase in Fe wire number should lead to increase the concentration of Fe vapor in the arc plasma zone where Fe nanoparticles are formed. It should be noted that the particle size of Fe nanoparticles did not significantly change because the growth rate and the resident time of the Fe vapor in the reaction field in the quenching zone inside the cathode is limited.[31] Instead, the number of Fe particles could increase with the higher Fe vapor concentration there. It is important to recognize by seeing Fig. 1(e) that the dispersion of Fe nanoparticles can be preserved during the calcination step to prepare the sulfonated acid catalysts (SO_3H/Fe-SWCNHs).

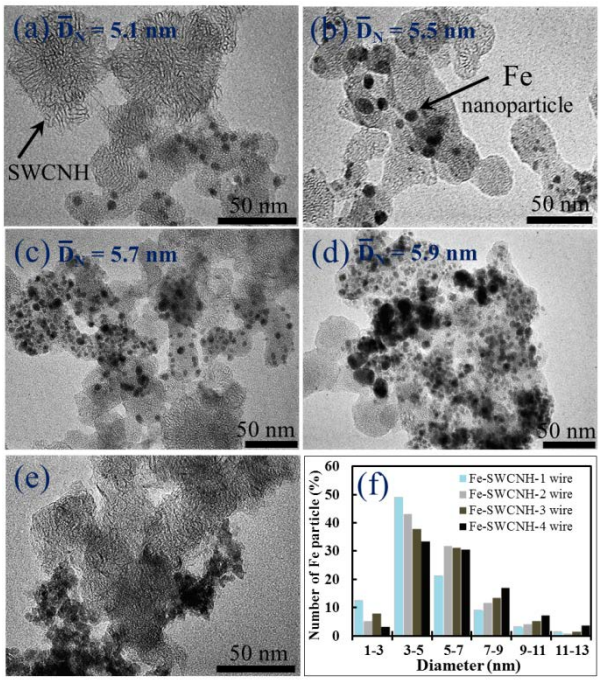

Fig. 1 TEM images of Fe-SWCNHs synthesized with various number of Fe wires, and mean diameters of Fe nanoparticles dispersed in Fe-SWCNHs. (a) 1 wire, (b) 2 wires, (c) 3 wires, (d) 4 wires. (e) TEM image of SO_3H/Fe-SWCNHs prepared by using Fe-SWCNHs synthesized with 4 Fe-wires. (f) Particle size distribution of Fe nanoparticle dispersed in Fe-SWCNHs.

We measured the Fe-loading amount in SWCNHs, and the result is plotted in Fig. 2 as function of number of Fe wires used in the synthesis process. It can be seen that the Fe-loading amount increases proportionally to the number of Fe wires.

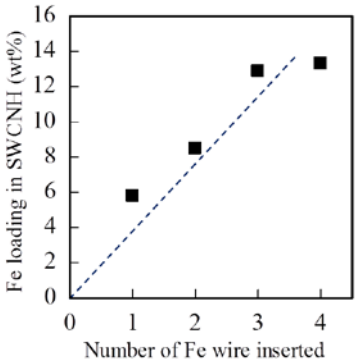

Fig. 2 Effect of number of Fe wires inserted in the anode hole in GI-AIW method on Fe-loading amount percentage in Fe-SWCMHs.

Transformation of Fe-SWCNHs to SO_3H/Fe-SWCNHs

The solid acid catalysts were prepared from Fe-SWCNHs by an impregnation method as experimental section. Since the acid site on these catalysts are considered to be -SO_3H,[32, 33] the catalysts prepared here are referred to as SO_3H/Fe-SWCNHs.

The crystal structure of Fe nanoparticles dispersed in Fe-SWCNHs was characterized by XRD. The diffraction patterns of Fe-SWCNHs were shown in Fig.3 in comparison with pure Fe powders and α-Fe_2O_3. The position of the diffraction peak of Fe-SWCNHs synthesized with four Fe wires well matches the diffraction peak of standard Fe at 45°. The other Fe-SWCNHs synthesized with one, two and three Fe wires also exhibit similar XRD patterns shown in Fig 3. This result confirms that the dark particles seen in the TEM images (Fig. 1) are Fe nanoparticles.

The XRD pattern of SO_3H/Fe-SWCNHs showed several peaks, although the intensities of the peaks should become fairly low because their crystal sizes are so small. The peak at 33° symbolized for Fe_2O_3 can be apparently seen in the XRD pattern of SO_3H/Fe-SWCNHs. Compared with this peak, other peaks of α-Fe_2O_3 at 35°, 40°, 54°could not be easily distinguished from baseline noise due to the small size of the crystals. In addition to the peak of Fe_2O_3, one must pay attention to the peak at 45°, representing ferromagnetic Fe. Although the peak at 45° is less prominent here than in Fe-SWCNHs, we consider that this XRD suggests that ferromagnetic Fe still remains in SO_3H/Fe-SWCNHs. It should be noted that SO_3H/Fe-SWCNHs can be captured by a permanent magnet as observed by using a neodymium magnet of surface magnetic flux 150 mT. The XRD result suggesting the inclusion of ferromagnetic Fe is consistent with this magnetic experiment.

The peak around 26º should come from carbonaceous parts in SO_3H/Fe-SWCNHs. The slight shift of this peak to lower angle and the appearance of new peaks at 24 º and 30 º may be caused by doping of S in structures consisting of C, Fe and O. Detail analysis on the structures pointed by these peaks are not the scope of this work, but it should be done in future.

Here, it should be informed that the most of metallic nanoparticles dispersed in SWCNHs produced by GI-AIW method are migrated in their carbonaceous part.[29] From this structural feature, it can be considered that the carbonaceous part in SO_3H/Fe-SWCNHs should be partially oxidized to become porous so that O_2 can diffuse through the carbonaceous part to reach Fe nanoparticles in Fe-SWCNHs. According to this pore opening effect, Fe nanoparticles migrated in SWCNHs could be transformed to α-Fe_2O_3.

It was found that this morphological change with opening pores on carbonaceous part was affected by the Fe-loading amount. Table 1 shows the BET specific surface area of SO_3H/Fe-SWCNHs, $S_{S,catal}$, synthesized with the varied Fe-wire numbers. Because the loading weight of the high-density Fe became larger when the Fe-wire number is larger, the specific surface area of SO_3H/Fe-SWCNHs became lower accordingly. Here, it should be emphasized that the specific surface area of the carbonaceous parts in SO_3H/Fe-SWCNHs, $S_{s,c}$, also decrease with the Fe-loading amount. The value of $S_{s,c}$ was calculated by Eq. (1) with an assumption that the exposed surface area of Fe_2O_3 could be negligible in comparison with carbonaceous part.

$$S_{s,c} = S_{catal}\, W_{catal} / (W_{catal} - W_{Fe2O3}) \quad (1)$$

where W_{catal}, and W_{Fe2O3} are mass of SO_3H/Fe-SWCNHs and Fe_2O_3 in SO_3H/Fe-SWCNHs. W_{Fe2O3} was measured by removal of carbonaceous part via thorough oxidation. SO_3H-SWCNH without Fe was also prepared for comparison. Note that the acid functional group cannot be impregnated well on SWCNH surface without Fe dispersion as shown in Table 1.

It is reported that pores can be opened on pure-carbon SWCNH by calcination in air.[34] In the case of SO_3H/Fe-SWCNH, Fe could catalyze the oxidation of the carbonaceous parts so that the inclusion of larger Fe-loading amount could lead to widen the pores. The average micropore diameter determined by *t*-plot method, d_m, is also shown in Table 1. It can be seen that d_m increases with Fe-loading amount. The relatively wide pores generated with the large Fe-loading amount could contribute to the stable re-usability of SO_3H/Fe-SWCNHs as explained in the subsequent section.

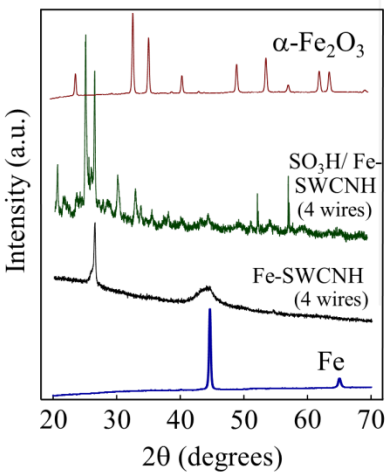

Fig. 3 XRD patterns of Fe powder, Fe-SWCNH, SO_3H/Fe-SWCNH synthesized with 4 wires of Fe and α-Fe_2O_3 powder.

Table 1 Acid site concentration, BET surface area, and average micro pore diameter of SO_3H/Fe-SWCNHs synthesized by inserting various number of Fe wires

Catalyst	Acid site concentration [a] (H^+-mmol g^{-1})	$S_{s,catal}$ [b] (m^2 g^{-1})	$S_{s,c}$ [c] (m^2 g^{-1})	d_m [c] (nm)
SO_3H-SWCNH (without Fe)	0.15	---	749	0.41
SO_3H/Fe-CNH (1wire)	5.6	68	79	0.68
SO_3H/Fe-CNH (2wire)	8.5	49	60	0.70
SO_3H/Fe-CNH (3wire)	7.5	18	23	0.75
SO_3H/Fe-CNH (4wire)	8.1	9	11	0.79

[a] Calculated by titration experiment.
[b] Determined based on unit mass of SO_3H/Fe-CNH.
[c] Determined based on unit mass of carbon part.

As shown in Table 1, the resultant SO_3H/Fe-SWCNHs can possess high acid site concentration of 5.6-8.5 mmol g^{-1}, which is comparable with that of sulfonated solid superacid catalysts previously reported.[35] Therefore, SO_3H/Fe-SWCNH prepared in this work can be accounted for super acid catalyst. It should be noted that no acid site was detected on Fe-SWCNHs without impregnation process. The average acid site concentration obtained from all SO_3H-Fe/SWCNHs specimen is 7.4 mmol/g. The relative error to obtain the acid site concentration estimated by repeated analysis informed us to be the level of 20%. According to the possible error,

the acid site density measured in the present work is considered to be independent of the wire number used in the synthesis process.

Effect of Fe-loading amount on catalytic activities for esterification

In this work, the effect of Fe-loading amount on catalytic activity for esterification of palmitic acid was investigated using SO_3H/Fe-SWCNHs synthesized with varied Fe-wire numbers. In order to assure the fair comparison, the amount of SO_3H/Fe-SWCNHs which were supplied into the reactor was adjusted so that the amount of acid sites used in each batch is supposed to be the same. The change of the methyl palmitate yield by SO_3H/Fe-SWCNHs with different Fe-loading amount is shown in Fig. 4 as a function of reaction time. It can be observed that the yield increases with increasing of Fe-wire numbers used for the synthesis process. It means that the increase of Fe-loading amount can enhance the catalytic activities in esterification of palmitic acid.

The reason of this enhancement effect of the Fe-loading can be discussed by considering the role of the Fe/Fe_2O_3 nanoparticles dispersed in SO_3H/Fe-SWCNHs. It is known that Fe_2O_3 has high affinity with carboxylic acid, including fatty acids like palmitic acid.[24] Therefore, palmitic acid can be first adsorbed by Fe_2O_3 surface at SO_3H/Fe-SWCNHs. Then, the adsorbed palmitic acid could diffuse to the acid sites (SO_3H-) anchored on the carbonaceous part. It can be considered that the enrichment of palmitic acid on Fe_2O_3 would be so significant that the amount of the access of palmitic acid to the acid sites via the Fe_2O_3 surface could become so large. We consider that such access via the Fe_2O_3 could be comparable with the direct access.

The yield of methyl palmitate at 60 min reaction time is plotted against the Fe-loading weight percentage in Fig. 5 to clarify the relation of the Fe-loading amount to the catalytic activity of SO_3H/Fe-SWCNHs. It can be clearly observed that the yield at 60 min is nearly proportional to the Fe-loading weight percentage, by which the yield reaches 92% at the highest Fe-loading of 13 wt%.

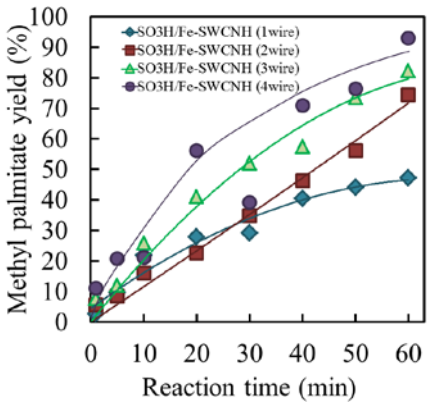

Fig. 4 Methyl palmitate yield obtained by esterification of palmitic acid with SO_3H/Fe-SWCNHs synthesized with varied Fe-wire numbers. (The reaction conditions: methanol/palmitic acid mass ratio of 33:1, amount of acid site at 1.1 mmol reaction temperature of 64°C, total reaction time of 60 min.)

The catalytic performance of a conventional sulphuric acid catalyst for the esterification of palmitic acid with the same condition can be referred from our previous work[36]. The methyl palmitate yield by the conventional catalyst was 20% in 60 min. In comparison, the yield obtained by SO_3H/Fe-SWCNHs catalyst synthesized in the present work became almost five times as high as by the conventional one.

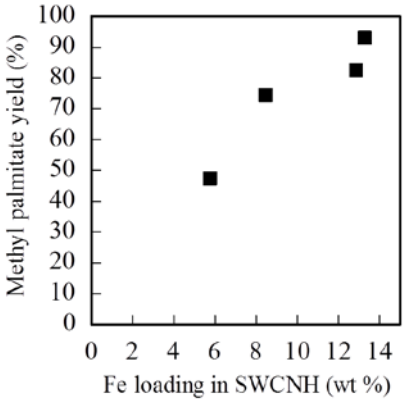

Fig. 5 Effect of Fe-loading amount on the maximum methyl palmitate yield in 60 min of reaction time

Reusability of catalysts in the esterification

The stability of the catalytic activity of SO_3H/Fe-SWCNHs against the reuse was investigated. The detail of this procedure is explained in the experimental section. The results are depicted in Figs. 6 and 7. As presented in Fig. 6, SO_3H/Fe-SWCNHs synthesized with Fe-wire number of 4 exhibits the excellent reusability in esterification. The yield slightly decreased by 5% in three reaction cycles. In the cases of SO_3H/Fe-SWCNHs synthesized with Fe-wire numbers of 1, 2 and 3, the yield decreased by 10-30%. This catalyst deactivation may be caused from the pore plugging by the adsorbed palmitic acid molecules, which limits their access to the acid sites. As mentioned previously, Fe-loading could widen the pores. Thus, the plugging would not occur when Fe-loading amount was so large in the case of Fe-wire number of 4.

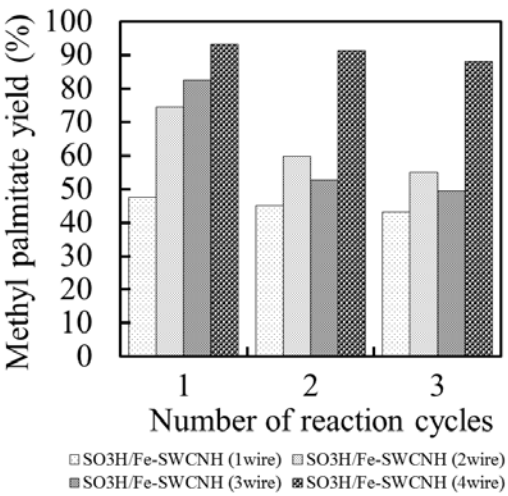

Fig. 6 Reusability of SO_3H/Fe-SWCNHs synthesized with various number of Fe wires for the esterification of palmitic acid with methanol. (The reaction condition was as same as mentioned in Fig. 5)

Magnetic property for re-use of SO_3H/Fe-SWCNHs

The stability of magnetic property of SO_3H/Fe-SWCNHs against the reuse for the esterification reaction was investigated as shown in Fig. 7. In this figure, the results obtained from SO_3H/Fe-SWCNHs synthesized with varied Fe-wire numbers are shown, and monotonous trend in the magnetic property in accordance with the Fe-wire number is not seen. Fig. 7(a,b) shows the AC magnetic susceptibility of SO_3H/Fe-SWCNH before they were used for the esterfication experiment, and Fig. 7(c,d) shows the AC magnetic susceptibility after the reuse of 1-3 times. The influence of the reuse of SO_3H/Fe-SWCNHs on their magnetic property can be evaluated by comparison between (a,b) and (c,d). It can be seen that the influence of the reuse on the AC magnetic susceptibility of SO_3H/Fe-SWCNHs is not significantly changed for all Fe-wire numbers in all the frequency range, in which the AC magnetic susceptibility is not decreased remarkably by the reuse of SO_3H/Fe-SWCNHs to catalyze the esterification reaction. Namely, the magnetic property of Fe/Fe_2O_3 dispersing in SO_3H/Fe-SWCNHs did not leach out during the esterification reaction.

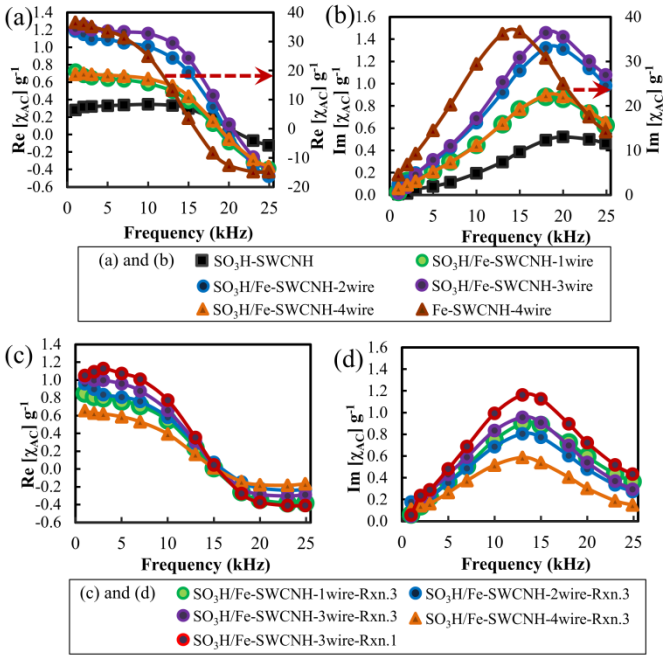

Fig. 7 AC magnetic susceptibility (χ_{AC}) of as-prepared Fe-SWCNH (4wire) and SO_3H/Fe-SWCNHs obtained from synthesis process with different Fe wire numbers as function of frequency of AC magnetic field (15mG) applied on specimen. Re[χ_{AC}] and Im[χ_{AC}] denotes the real and imaginary parts of the complex number of χ_{AC}, respectively. (a) and (b) show the AC magnetic susceptibility of SO_3H/Fe-SWCNHs before use for esterification experiment, and (c) and (d) show the magnetic susceptibility after use for the esterification experiment. Rxn in (c) and (d) means the number of repetition for the esterification experiment.

Conclusions

Fe-SWCNHs were used as starting materials for preparing sulfonated SWCNHs by acid impregnation method. It was found that the Fe-loading amount was proportional to the number of Fe-wire in the anode by GI-AIW method, and the Fe-loading amount became 6-13 wt% in the present conditions.

It was observed that SO_3H/Fe-SWCNHs possessed high acid site concentration of 5.6-8.5 mmol g^{-1}, which can be regarded as super acid solid catalyst. The most of Fe nanoparticles dispersed in SO_3H/Fe-SWCNHs were oxidized to cause transformation to α-Fe_2O_3 during a calcination step. Nevertheless, trace of Fe remaining there can have a roll to realize magnetic recovery of SO_3H/Fe-SWCNHs using a permanent magnet.

The catalytic activity of SO_3H/Fe-SWCNHs for esterification of palmitic acid with methanol was investigated. The results clearly show that high amount of Fe loading provides high yield of methyl palmitate because the presence of Fe/Fe_2O_3 can enhance the adsorption of palmitic acid molecules on the surface of Fe_2O_3 nanoparticles. Then, the enriched palmitic acid molecules could diffuse to the acid sites. In addition, the reusability of SO_3H/Fe-SWCNHs was revealed that the deactivation of catalytic activity of SO_3H/Fe-SWCNHs is significantly reduced when Fe-loading amount is large enough. It is noteworthy that the magnetic susceptibility of SO_3H/Fe-SWCNHs can be preserved when SO_3H/Fe-SWCNHs are repeatedly used.

From a sustainability point of view, first, the catalyst prepared here does not use any rare metals which are sometimes used to prepare the catalyst for biofuel synthesis,[37] although high capacity of strong acid site is realized. Moreover, our catalyst can be recovered from the solution simply by using a permanent magnet. Only a little energy is required for this recovery system. One may worry that synthesis of SWCNHs by arc discharge method is energy intensive and costly. Related with this issue, it is reported that the cost to produce SWCNHs can be reduced by two order by optimization of the reaction condition when moderate purity of electrode is employed.[38] In addition, new route to synthesize SWCNHs at relatively low temperature is explored.[39] Thus, we expect that the energy-base yield to prepare the catalyst proposed here may be significantly improved by further optimization.

Experimental methods

Synthesis of Fe-SWCNHs by arc discharge method

Single-walled carbon nanohorns dispersed with Fe nanoparticles (Fe-SWCNHs) were synthesized by N_2 gas injected arc-in-water (GI-AIW) method.[30] The set-up and dimensions of the reaction system of this method is illustrated in Fig. 8. A cathode and an anode were high purity graphite rod (99.9995%). Various number (from 1 to 4) of the Fe wires (0.5 mm in diameter) were inserted in the anode hole drilled along its axis. Both electrodes were submerged in water at room temperature. To generate arc discharge, DC current was supplied to the electrodes by a welding machine (Shindaiwa, STW200A) at 80 A and 40 V. For continuous arc discharge, the anode was delivered along the axis of cathode hole with a speed of 1 mm/s. The N_2 gas was injected into the arc plasma zone inside the cathode hole by 10 L/min when arc discharge was generated for 1 min. By this condition, Fe-SWCNHs were synthesized and collected from water surface finally.

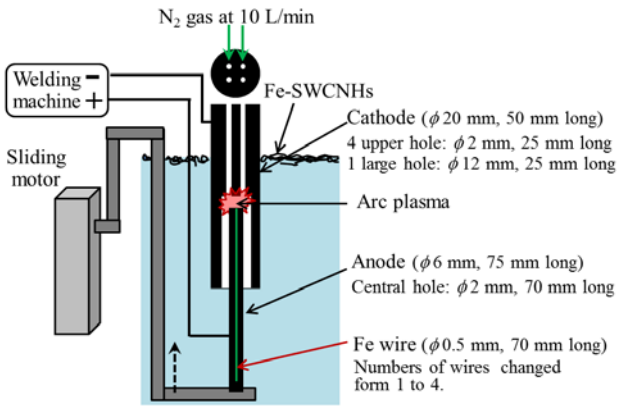

Fig. 8 Set-up apparatus for synthesis Fe-SWCNHs, and dimensions of cathode, anode and Fe wires

Determination of Fe-loading amount (wt%) in Fe-SWCNHs

As-grown Fe-SWCNHs were oxidized by ambient air in an open-end quartz tube placed in an electric furnace at 900°C for 30 min. All carbonaceous parts were oxidized, and only reddish brown powders remained there. XRD analysis was used to confirm that the reddish brown powders were Fe_2O_3, and no carbon was detected. The weight of the remaining Fe_2O_3 was measured, and then Fe-loading amount (wt%) in Fe-SWCNHs was calculated.

Synthesis of SO_3H/Fe-SWCNHs catalyst by impregnation method

As-grown Fe-SWCNHs prepared by the GI-AIW method with various Fe-wire numbers were immerged in concentrated sulphuric acid (95%) for 24 h. After acid impregnation, Fe-SWCNHs were washed by distilled water for three times and then dried in an oven with ambient air at 110°C for 12 h. Finally, Fe-SWCNHs were calcined in furnace with air supply of 10 L/min at 400°C for 3 h. The resultant sulfonated Fe-SWCNHs (SO_3H/Fe-SWCNHs) were obtained and kept in vacuum desiccator.

Morphology characterization of Fe-SWCNHs and SO_3H/Fe-SWCNHs catalyst and size distribution of Fe nanoparticles

The morphologies of the as-grown Fe-SWCNHs and SO_3H/Fe-SWCNHs were analysed by a transmission electron microscope (TEM) (JEOL, JEM-1010). The size distributions of Fe nanoparticles dispersed in Fe-SWCNHs were determined by measuring the diameters of 500 particles of Fe nanoparticles in TEM images.

X-ray diffraction analysis

The X-ray diffraction patterns were recorded by a X-ray diffratometer (Ringaku, Ultima IV 285 DX) with Cu Kα radiation from 40kV and 20 mA. The pure Fe and Fe_2O_3 powders were also analyzed to compare peak positions with the catalyst.

Magnetic property analysis

Analysis of the magnetization in Fe-SWCNH and SO_3H-Fe-SWCNH were carried out by measuring AC magnetic susceptibility at room temperature with a maximum magnetic flux 15 mG (Magqu Co., XacQuan-II).

Acid site concentration of SO_3H-Fe-SWCNH catalysts

The acid site concentrations of the catalysts were determined by acid base titration using standard NaCl solution as an ion-exchange agent. The 5.0 ml of 2.0 M NaCl ion-exchanged with 25 mg of the catalyst specimen under agitation (150 rpm) for 24 h was titrated with 0.01 M NaOH solution. Phenolphthalein was used to detect the equivalence point.

Catalytic activity analysis by esterification of palmitic acid

The catalytic activities of SO_3H/Fe-SWCNHs were evaluated by a liquid phase esterification of palmitic acid with methanol as follows. A 100 ml three-necked flask equipped with a water condenser was used as a reactor. This flask was submerged in an oil bath of which temperature was controlled by a stirring heater. Also the solution in the flask was stirred by a magnetic bar. Powdery palmitic acid (1.28 g) was placed into this reactor, and its melting was waited. When the palmitic acid became clear solution at 64°C, 5.27 g of warm methanol (99.8%) was added into reactor. After that, the catalysts were added into the reactor with same amount of acid site at 1.1 mmol. The reaction temperature was controlled at 64°C and the reactants were well mixed under agitation of 600 rpm for 60 min. The methyl palmitate produced from the esterification reaction was collected periodically to measure its concentration by a gas chromatograph (Shimadzu, GC-14B). Ar was used as the carrier gas through a GC column (GL Science Ltd., Unisole 3000, 3 mm in diameter and 2 m in length) and a flame ionization detector. The methyl palmitate yield (Y, %) was determined according to the equation (1).

$$Y\,(\%) = \frac{mole\ of\ methyl\ palmitate\ formed}{theoretically\ expected\ mole\ of\ methyl\ palmitate} \times 100 \quad (2)$$

Reusability of SO_3H-Fe-SWCNH catalyst

The stability of the catalytic activity of SO_3H/Fe-SWCNHs against the reuse after the esterification of palmitic acid was investigated. To reuse the SO_3H/Fe-SWCNHs remaining in the reaction solution, SO_3H/Fe-SWCNHs were separated from the solution by a permanent magnet with surface magnetic flux of 150 mT. The catalysts were washed by methanol for three times and dried in air. The catalysts were then used for a new batch of esterification to start the next reaction cycle. The reusability was evaluated by the determination of the methyl palmitate yield at 60 min. In addition, the AC magnetic susceptibility of the reused catalysts was measured after using in every cycle.

Acknowledgements

This work was financially supported by a JSPS Postdoctoral Fellowship for Foreign Researchers FY 2012 and This work was financially supported by JSPS KAKENHI Grant Number 24360327.

Notes and references

1. J. A. Melero, J. Iglesias and A. Garcia, *Energ Environ Sci*, 2012, **5**, 7393-7420.
2. G. Koçar and N. Civaş, *Renewable Sustainable Energy Rev.*, 2013, **28**, 900-916.

3. D. M. Alonso, J. Q. Bond and J. A. Dumesic, *Green Chem.*, 2010, **12**, 1493-1513.
4. R. Luque, J. C. Lovett, B. Datta, J. Clancy, J. M. Campelo and A. A. Romero, *Energ Environ Sci*, 2010, **3**, 1706-1721.
5. E. E. Kwon, J. Seo and H. Yi, *Green Chem.*, 2012, **14**, 1799-1804.
6. S. Pinzi, I. L. Garcia, F. J. Lopez-Gimenez, M. D. L. de Castro, G. Dorado and M. P. Dorado, *Energy Fuels*, 2009, **23**, 2325-2341.
7. D. Y. C. Leung, X. Wu and M. K. H. Leung, *Appl. Energy*, 2010, **87**, 1083-1095.
8. H. Fukuda, A. Kondo and H. Noda, *J. Biosci. Bioeng.*, 2001, **92**, 405-416.
9. G. L. Maddikeri, A. B. Pandit and P. R. Gogate, *Ind. Eng. Chem. Res.*, 2012, **51**, 14610-14628.
10. P. Sinthupinyo, H. Habaki and R. Egashira, *J. Chem. Eng. Jpn.*, 2010, **43**, 214-223.
11. M. G. Kulkarni and A. K. Dalai, *Ind. Eng. Chem. Res.*, 2006, **45**, 2901-2913.
12. A. Emil, Z. Yaakob, M. N. S. Kumar, J. M. Jahim and J. Salimon, *J. Am. Oil Chem. Soc.*, 2010, **87**, 689-695.
13. J. A. Melero, J. Iglesias and G. Morales, *Green Chem.*, 2009, **11**, 1285-1308.
14. S. H. Shuit, K. F. Yee, K. T. Lee, B. Subhash and S. H. Tan, *Rsc Adv*, 2013, **3**, 9070-9094.
15. K. Nakajima and M. Hara, *Acs Catal*, 2012, **2**, 1296-1304.
16. L. J. Konwar, J. Boro and D. Deka, *Renewable Sustainable Energy Rev.*, 2014, **29**, 546-564.
17. Zillillah, G. Tan and Z. Li, *Green Chem.*, 2012, **14**, 3077.
18. C. Perego and R. Millini, *Chem. Soc. Rev.*, 2013, **42**, 3956-3976.
19. X. Duan, Y. Liu, Q. Zhao, X. Wang and S. Li, *Rsc Adv*, 2013, **3**, 13748.
20. G. Paterson, T. Issariyakul, C. Baroi, A. Bassi and A. Dalai, *Catal. Today*, 2013, **212**, 157-163.
21. K. Wilson and A. F. Lee, *Catal. Sci. Technol.*, 2012, **2**, 884.
22. T. M. Sankaranarayanan, R. V. Shanthi, K. Thirunavukkarasu, A. Pandurangan and S. Sivasanker, *J. Mol. Catal. A: Chem.*, 2013, **379**, 234-242.
23. B. Kollbe Ahn, H. Wang, S. Robinson, T. B. Shrestha, D. L. Troyer, S. H. Bossmann and X. S. Sun, *Green Chem.*, 2012, **14**, 136.
24. M. Cano, K. Sbargoud, E. Allard and C. Larpent, *Green Chem.*, 2012, **14**, 1786-1795.
25. K. Ullah, M. Ahmad, S. Sultana, L. K. Teong, V. K. Sharma, A. Z. Abdullah, M. Zafar and Z. Ullah, *Appl. Energy*, 2014, **113**, 660-669.
26. G. S. Macala, A. W. Robertson, C. L. Johnson, Z. B. Day, R. S. Lewis, M. G. White, A. V. Iretskii and P. C. Ford, *Catal. Lett.*, 2008, **122**, 205-209.
27. S. Zhu and G. Xu, *Nanoscale*, 2010, **2**, 2538-2549.
28. N. Sano, T. Ishii, H. Mori, Y. Ikeyama and H. Tamon, *J. Appl. Phys.*, 2012, **112**, 044301.
29. C. Poonjarernsilp, N. Sano, T. Charinpanitkul, H. Mori, T. Kikuchi and H. Tamon, *Carbon*, 2011, **49**, 4920-4927.
30. N. Sano, *J Phys D Appl Phys*, 2004, **37**, L17-L20.
31. C. Poonjarernsilp, N. Sano, H. Tamon and T. Charinpanitkul, *J. Appl. Phys.*, 2009, **106**, 104315.
32. R. Xing, Y. M. Liu, Y. Wang, L. Chen, H. H. Wu, Y. W. Jiang, M. Y. He and P. Wu, *Microporous Mesoporous Mater.*, 2007, **105**, 41-48.
33. K. Hou, A. Zhang, L. Gu, M. Liu and X. Guo, *J. Colloid Interface Sci.*, 2012, **377**, 18-26.
34. N. Sano, Y. Akita and H. Tamon, *J. Appl. Phys.*, 2011, **109**, 124305.
35. P. Chen, M. Du, H. Lei, Y. Wang, G. Zhang, F. Zhang and X. Fan, *Catal. Commun.*, 2012, **18**, 47-50.
36. C. Poonjarernsilp, N. Sano and H. Tamon, *Appl. Catal., B*, 2014, **147**, 726-732.
37. A.E. Barron Cruza, J.A. Melo Banda, Hernandez Mendoza, C.E. Ramos-Galvan, M.A. Meraz Melo and D. Esquivel, *Catal. Today*, 2011, **166**, 111–115.
38. N. Sano, Y. Yasumura, Y. Kimura, A. Toyoda and K. Hirano, *Trans. MRS Jpn*, 2008, **33**, 669-672.
39. N. Sano, T. Ishii and H. Tamon, *Carbon*,2011, **29**, 3698–3704.